

Power Performance of Stirling Motors Driven from Modified Orgone Accumulators

Paulo N. Correa, Alexandra N. Correa, and Eugene Mallove

Abstract

We have previously reported on the application of modified (or hybrid) Orgone Accumulators, referred to as HYBORACs, to serve as day and nighttime drives for low delta-T Stirling engines.^{1,2} We now report on calibrated power determinations of the mechanical output of MM6 Stirling engines, performed with a string-and-pulley method and with a sensitive prony-brake dynamometer, and we compare these to the predictions from Schmidt theory for Stirling engines. For a near 20.5 hours continuous running—8 hours of which was during nighttime—the HYBORAC/Stirling assembly output 6.12 kJ, with a daytime power mean of 125 mW and a nighttime output power mean of 25 mW. Peak output power reached 165 mW.

Introduction

Simple sheet metal Faraday cages have been shown to be able to sustain positive temperature differences (To-T) with respect to their adjacent surrounding atmosphere, even under stringently controlled indoor dark basement conditions designed to minimize those differences.³ (Here To refers to the temperature taken either above the top surface of the Faraday cage—usually within 1 to 2 cms of the top—or inside of it, near 2 cms below the top, and T is air temperature adjacent to the Faraday cage as measured by a suspended mercury thermometer, typically 30 cm laterally from the cage.) This anomalous thermal phenomenon was first discovered by W. Reich and later effectively confirmed by A. Einstein,³ though unfortunately he accepted his assistant L. Infeld's quite erroneous attribution of the positive (To-T) to air convection currents. Because of the astonishing and revolutionary nature of this discovery by Reich, which is the groundwork for the present paper, it is important to summarize the non-scientific response of these "authorities" to the experiment: Einstein and Infeld pursued *no further experimental studies*, despite detailed critiques by Reich of their objections. This unscientific behavior would begin to characterize physicists' approaches to other challenging phenomena in the twentieth century, such as electrodynamic explosions and Low-Energy Nuclear Reactions (LENR), with their associated excess heat phenomena.

However, to develop from this (To-T) phenomenon a useful application that simultaneously permits a clear demonstration of the temperature differences and utilizes them to generate work, one must optimize the physical conditions that generate sensible heat inside and atop these cages, so as to make To-T as large as possible. W. Reich opened the way in this direction when 1) he insulated these cages to create

what he termed Orgone Accumulators (ORACs) by employing special materials for their construction and layering alternating metal and thermally insulating materials, and then 2) proceeded to measure the temperature difference outdoors where he found that "It increases and decreases with the intensity of solar radiation."⁴ This led him to directly expose these ORACs outdoors to solar radiation, having found that "on summer days, under a strong sun, (To-T) dif-

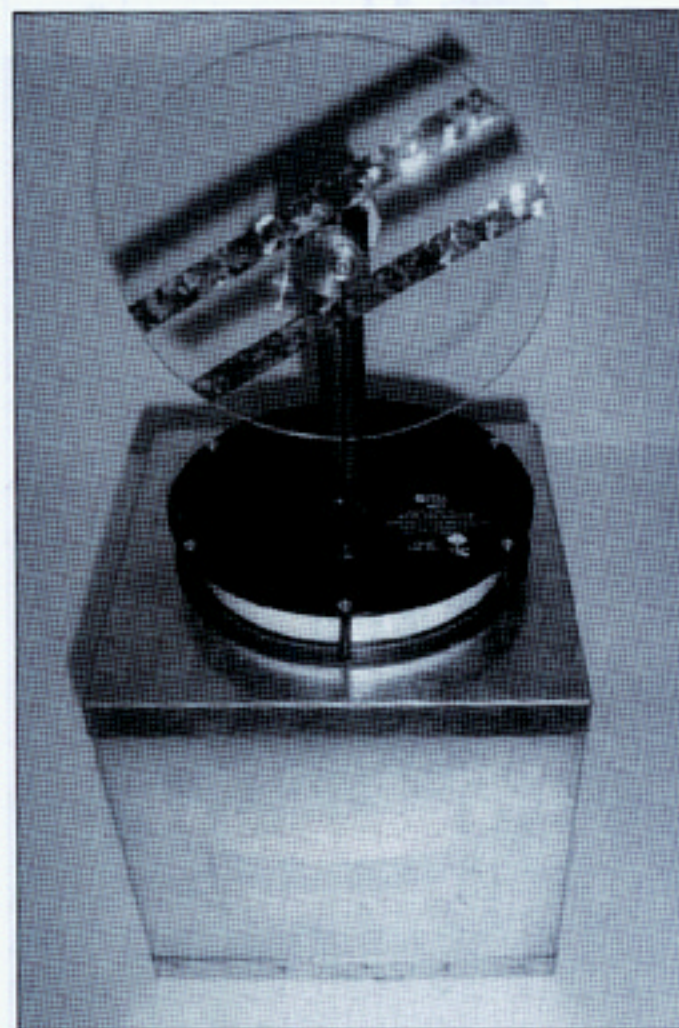


Photo 1. Front and top view of an MM6 Stirling engine resting on top of an 8 inch cube Faraday cage. In the HYBORAC/Stirling experiments performed in the Toronto, Canada area in May 2003, a similar 8-inch cube Faraday cage was employed.

ferences up to 20°C are not uncommon."⁵ Despite Reich's clear attribution of "atmospheric and ground orgone radiation" to the sun:

If the radiation in question [*i.e.* orgone energy] were directly connected with solar energy, then many phenomena could be easily explained. . . Furthermore, [orgone] is radiated into the atmosphere by the sun and is therefore present everywhere. . .⁶

Despite even his explicit claim that he had "proof of its solar origin,"⁴ self-styled Reichian followers have shrunk from confirming this proof, as much as from studying the effects of direct solar radiation upon ORACs.⁷ It was the first two authors of this paper, in fact, who penned the first such scientific study,⁸ demonstrating, with both ample experimental evidence and new analytical tools, how solar radiation consists fundamentally of what they appropriately described and named *massfree, longitudinal, ambipolar (electric) energy*, and identifying its exact energy spectrum.^{9,10} The same two authors have also identified the modal spectra of IR (infra-red) photon absorption for black ORACs (peaks at 42.5 μm wavelength) and white ORACs (peaks at 45 μm wavelength) under solar exposure—and formally demonstrated how very-long wavelength IR absorption cannot in

any way account for the sensible thermal energy generated inside these ORACs. This put to rest the spurious contentions of certain Reichians (*e.g.* J. DeMeo⁷) who believe that the thermal anomaly is caused by IR absorption.

We have, in a previous publication, proposed a model for the evolution of sensible heat (blackbody photons) inside Faraday cages and ORACs.² Essentially, solar-atmospheric ambipolar radiation is captured by electronic and atomic matter, to which it confers kinetic energy (in the sense of the kinetic theory of gases, as energy of translatory motion), and loss of the latter results in the production of blackbody photons through specific aetherometric transformations.⁹ However, ambipolar radiation can also be captured to confer *latent heat*—*i.e.* increase the energy content of "the atmospheres of molecules," or their "latent heat of phase change." This production of latent heat is, in fact, the dominant pathway, but has not been understood by "accepted physics" for reasons that are now all too clear. Undoubtedly the energy states to which "latent heat" refers are also kinetic energy states, but they are not normally understood as such because they relate to structural features—such as Van der Waals or noncovalent bonds and molecular phase states—that are thought to involve rotary or vibratory motions. In turn, this more comprehensive and accurately defined latent heat can also be released to produce blackbody photons.

Previous determinations¹¹ estimated the quantity of latent heat present inside black ORACs (BORACs) and sustaining a $T_o - T = 10^\circ\text{C}$, to be at least 3x greater than the accompanying quantity of sensible heat. Modification of these BORACs was undertaken to maximize their $T_o - T$ values both under direct solar exposure¹ and in total darkness,² by hybridizing them with matté-black special Faraday cages to create the HYBORAC design, with its two configurations—daytime and nighttime.²

The present communication reports on the mechanical power calibration studies of the MM6 Stirling engine, performed with sensitive spring-loaded prony-brake dynamometers. Other calibrations—with string-and-pulley, and quadrant and hung-weight prony-brake dynamometers—were also performed with similar results. These experimental tests were compared to the Schmidt theory of so-called γ -type Stirling engines—a class to which the MM6 belongs. The spring-loaded prony-brake dynamometer calibration was then employed to determine the mechanical output power of a typical experiment. To be precise, we measured the mechanical power of the Stirling engine mechanism as it expended energy against its own internal friction and resistance during steady state operating conditions—no additional loads external to the Stirling were employed in this study.

Note on Methods and Materials

With the exception of the string-and-pulley tests, which were performed on one particular low ΔT MM6 Stirling engine that was not coupled to a HYBORAC, all the experiments reported in the present communication employed the very same low ΔT MM6 Stirling motor (coded by us as "#2") made by the American Stirling Company in San Diego, California. (See Photos 1 and 2, showing side and front views.)

Results

Comparison of Faraday cages and ORACs exposed to solar-

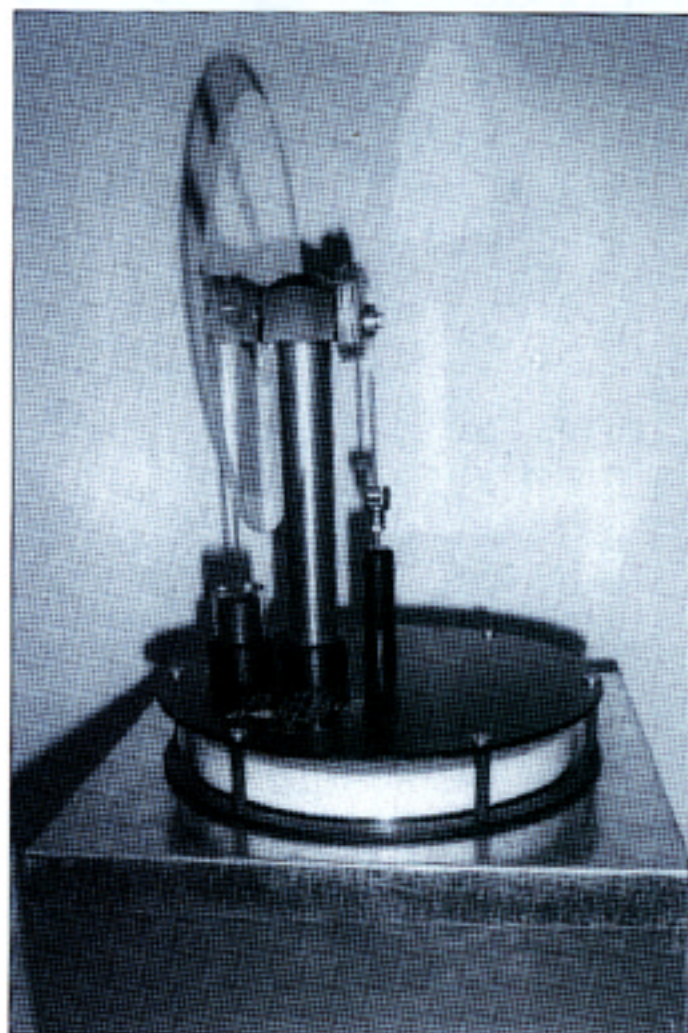


Photo 2. View of the MM6 Stirling engine used for weight-fall testing. Nylon thread wind-up spool, a slight modification to the MM6, is visible.

atmospheric radiation.

Early experiments identified evolution of much greater diurnal temperatures inside (2 cm below the top plate) matté-black Faraday cages than inside the inner chamber of 2x (*i.e.* interposed 2 metal and 2 insulating layers) matté-black ORACs (BORACs) having the same internal volume of 1 cubic foot, when both were directly exposed to solar-atmospheric radiation. The internal To-T values for these two apparatuses, together with the control values—for a metallic, uncoated Faraday cage of the same volume—are shown in Figure 1. Whereas the bare black Faraday cage reached To-T values of $\geq 30^{\circ}\text{C}$, when the BORAC only reached To-T values of 10 to 12°C , the BORAC was able to retain positive temperature differences longer into the nighttime, without letting the temperature difference turn negative. BORACs would reach 45°C with peak air temperatures of $30\text{--}35^{\circ}\text{C}$, while black Faraday cages would reach temperatures of 60 to 67°C , and up to 75°C on their outer top surface (so-called “heat waves” could readily be observed over the apparatus up to a height of 4 cm). The mean temperature values obtained from a comparative month-long study (during June and July, 1998) of their diurnal response outdoors were $40.45^{\circ}\text{C} \pm \text{SEM } 1.18^{\circ}\text{C}$ ($n=150$) for the black Faraday cage versus $34.26^{\circ}\text{C} \pm \text{SEM } 0.62^{\circ}\text{C}$ ($n=171$) for the BORAC. During the same period, a white-painted ORAC yielded a mean temperature of $27.13^{\circ}\text{C} \pm \text{SEM } 0.39^{\circ}\text{C}$. Mean air temperature was $25.56^{\circ}\text{C} \pm \text{SEM } 0.34^{\circ}\text{C}$ ($n=170$), clearly indicating that all experimental devices could sustain a net positive temperature difference around the clock, even if some (the control metal cage and the black Faraday cage) presented negative temperature differences during nighttime.

Most of the early thermal studies that we conducted—on both sensible and latent heats—employed the BORAC as standard.^{8,11} Even though the black Faraday cages performed better than the BORACs during daytime, they invariably led to null or negative temperature differences during nighttime.

From its onset, research and development of a hybrid of the two apparatuses—in the form of the HYBORAC design^{1,2}—was guided by the key objective of sustaining large temperature differences around-the-clock, even though at the time no heat was being extracted from these devices to feed a work process. In essence, we aimed at increasing not just the daytime To-T but, above all, the nighttime To-T values—beginning with avoidance of the negative temperature differences. Considerable progress was made, in this respect, in the earlier investigations—enough to subsequently permit continuous extraction of energy during daytime and for up to 6.7h during nighttime.^{1,2}

May 19, 2003 experiments

With the HYBORAC design described in our last report on this topic¹ and last tested during the late autumn days of 2002, we now sought to make a determination of its performance during spring. The daytime thermal difference values of the May 19, 2003 experiment are shown in Figure 2, and the corresponding nighttime values in Figure 3, with their respective DWLS (distance weighted least squares) curves. We need to introduce here ΔT , not to be confused with To-T! The ΔT refers to the temperature difference between the bottom plate (the “hot” plate) and the top plate (the “cold” plate) of the Stirling engine. Very high ΔT and To-T mean values of 17.7°C and 23.58°C , respectively, were

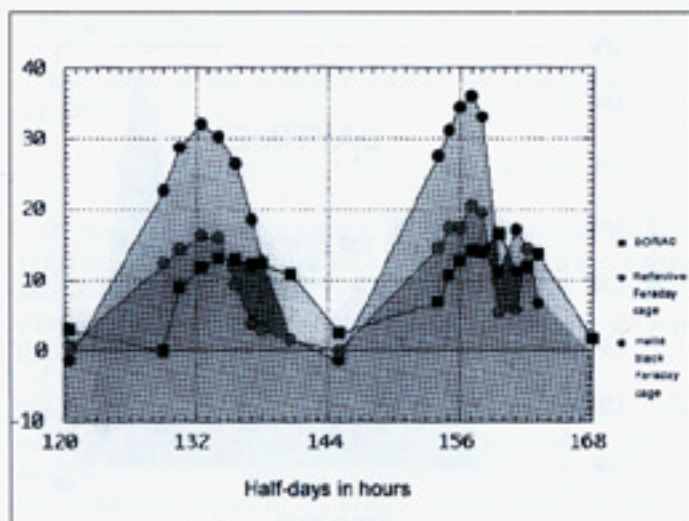


Figure 1. Internal To-T values for black ORAC (BORAC), for reflecting (bare) Faraday cage and for matté black (bare) Faraday cage.

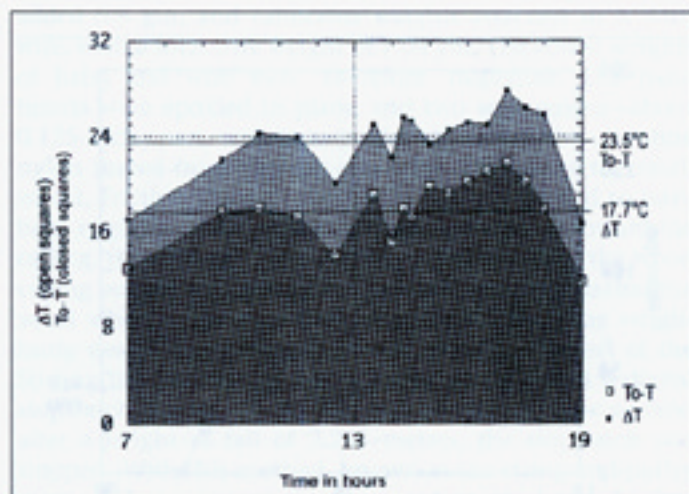


Figure 2. Thermal differences (daytime) for May 19, 2003 HYBORAC/Stirling testing. ΔT refers to the temperature difference between the bottom plate (the “hot plate”) and the top plate (the “cold plate”) of the Stirling engine. ΔT should not be confused with To-T difference, which pertains to upper HYBORAC surface temperature (To) references to ambient air temperature (T).

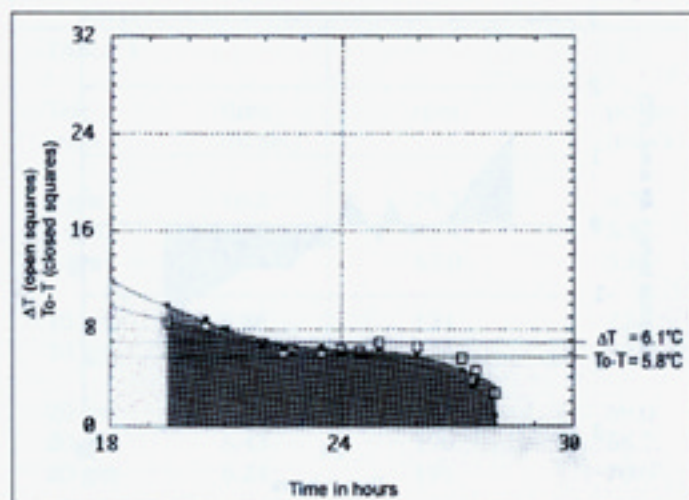


Figure 3. HYBORAC nighttime To-T and ΔT variation in the May 19-20, 2003 experiment. Note the inversion of the To-T and ΔT curves.

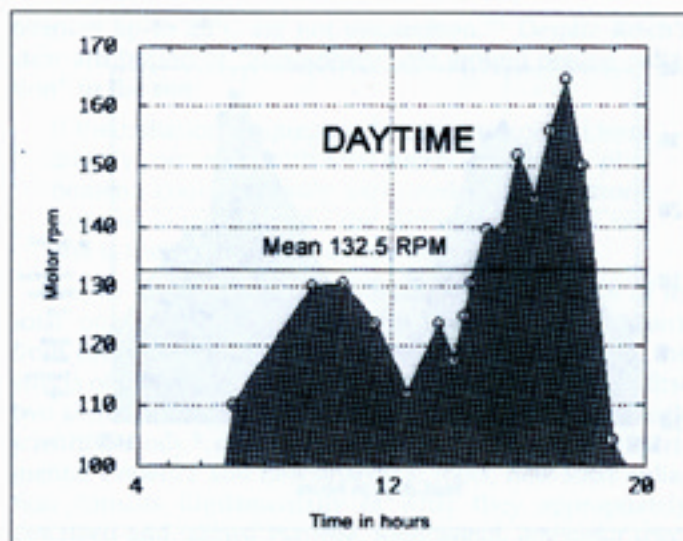


Figure 4. Stirling motor speeds (rpm) for daytime in the May 19, 2003 experiment.

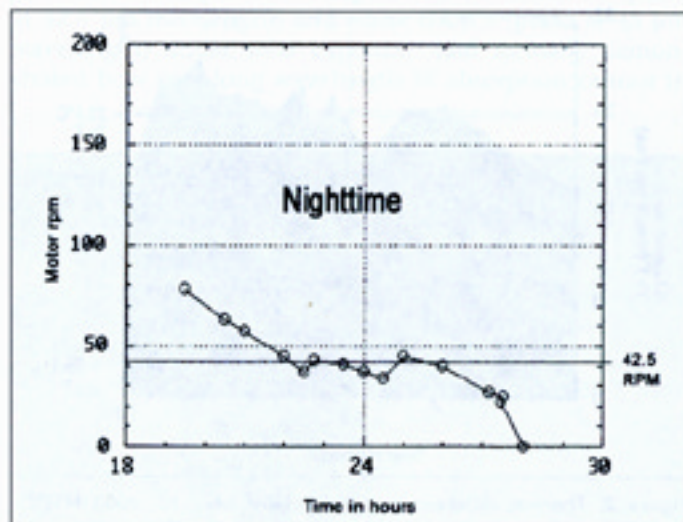


Figure 5. Stirling motor speeds (rpm) for nighttime in the May 19-20, 2003 experiment.

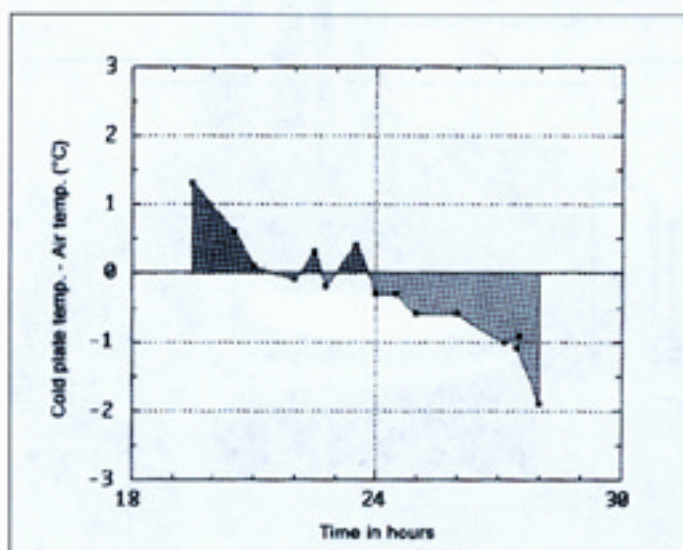


Figure 6. Nighttime inversion of the Stirling motor cold plate temperature with the control air temperature in the May 19, 2003 experiment.

registered during daytime, for a period of 12 hours; nighttime values, with means of $\Delta T = 6.1^\circ\text{C}$ and $T_o - T = 5.8^\circ\text{C}$ were solidly positive for 8 hours, until near 04:00 when $T_o - T$ abruptly decreased to 0.7°C . A typical inversion of the two curves (see Reference 2) was observed after midnight.

The corresponding motor speeds are shown in Figure 4 (for daytime) and in Figure 5 (for nighttime). Mean daytime rpm was 132.5, and mean nighttime rpm 42.5. The motor came to a stop after 03:37 in the morning of the next day, having been driven continuously for eight hours in the absence of solar radiation. The motor also ran continuously during the changeover (at 19:15) from the daytime to the nighttime HYBORAC configurations.

During the May 19 experiment we came very close to achieving round-the-clock motor action—the Stirling engine MM6 (#2) having worked continuously for 20.5 hours.

To progress further we needed to better understand the inversion between the ΔT and $T_o - T$ values that is characteristic of the cooling period, and repeatedly accentuated towards the end of the motor activity. The motor did not come to a stop because these values became negative; rather, the $T_o - T$ and ΔT values remained positive but decreased to a magnitude too low to drive the engine. Often this happened because of atmospheric condensation of humidity and its release of heat, with attendant rise of the dewpoint outside the boxes. This increased the air temperature and thus decreased $T_o - T$ further. It also increased—with a lag—the temperature of the engine's cold plate, thus decreasing ΔT . The inversion could, in fact, be spotted by the negative trend in the temperature of the cold plate with respect to the air control temperature (see Figure 6): their difference becomes negative 2 hours after the nighttime configuration is adopted, settles after midnight, and exacerbates when the motor comes to a stop.

Schmidt analysis of the MM6 work and power outputs.

Schmidt theory of Stirling engines¹² assumes the performance can be determined from a P-V diagram, once the volumes of the engine and its dynamic cavities are known (see Figure 7)—along with the mass of the working gas and the temperature difference $\Delta T = T_{in} - T_f$ between the engine plates. The expansion moment volume, V_E , and the compression moment volume, V_C , are treated, the former as a function of the swept volume, V_{SE} of the displacer-regenerator piston (also called the expansion piston), and the latter as a function of both swept volumes— V_{SE} and V_{SC} , the swept volume of the power piston (also called the compression piston):

$$V_E = [(V_{SE}/2)(1 - \cos x)] + V_{DE}$$

$$V_C = [(V_{SE}/2)(1 - \cos x)] + [(V_{SC}/2)[1 - \cos(x - dx)]] + V_{DC}$$

where V_{DE} and V_{DC} are the "dead space" volumes of the expansion and compression phases of the cycle, and dx the phase angle between the displacer and power pistons (90° in these engines). For the MM6, the maximum volume of the expansion moment can be easily measured to be 141.37 cm^3 . The swept and "dead space" volumes can also be determined by examining the internal geometry of the motor: $V_{SE} = 132.5 \text{ cm}^3$, $V_{SC} = 151.1 \text{ cm}^3$, $V_{DE} = 8.8 \text{ cm}^3$, and $V_{DC} = 18.6 \text{ cm}^3$ (at 0°). We also need to know the volume of the regenerator—which is the volume of the displacer piston—

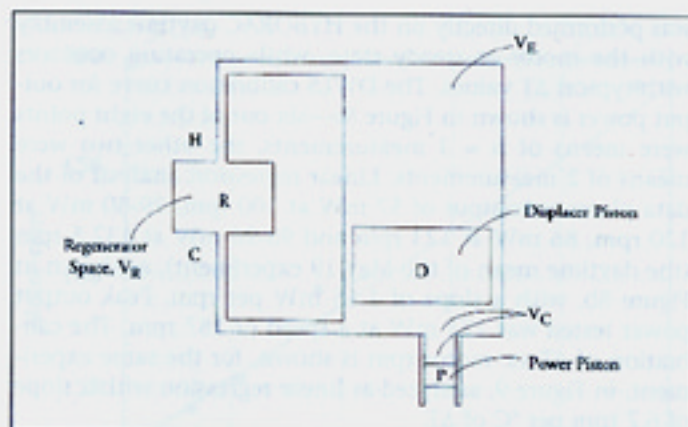


Figure 7. Schmidt interpretive model of the gamma-type Stirling engine.

and this, too, can easily be ascertained as $V_R = 247.4 \text{ cm}^3$.

To apply the Schmidt model¹² we need some other parameters that are specific ratios for temperature and volumes. We chose, for our inquiry, experimental data of a motor rpm mean of 118 rpm (1.967 rps), obtained outdoors with the HYBORAC/Stirling assembly in the daytime configuration, and a ΔT of 18.7°C . The temperature ratio t is:

$$t = T_f/T_{in} = 291.31 \text{ deg kelvin}/309.99 \text{ deg kelvin} = 0.9397$$

The swept volume ratio is $v = V_{SC}/V_{SE} = 1.14$, and the "dead" volume and regenerator ratios:

$$X_{DE} = V_{DE}/V_{SE} = 0.0667$$

$$X_{DC} = V_{DC}/V_{SE} = 0.1405$$

$$X_R = V_R/V_{SE} = 1.8666$$

From these parameters we then extract the values of the Schmidt functions: for the working angle a :

$$a = \tan^{-1} [(v \sin dx)/(t + \cos dx)] = 50.5^\circ$$

and for the Schmidt functions S , B and C :

$$S = t + 2tX_{DE} + [(4tX_R)/(1+t)] + v + 2X_{DC} + 1 = 7.111$$

$$B = [t^2 + [2(t-1)v \cos dx] + v^2 - 2y + 1]^{0.5} = 1.142$$

$$C = B/S = 0.1606$$

With these data, a P-V Schmidt diagram for the γ -type Stirling engine can be built, where the occupied P-V area corresponds to the work integrals for work-equivalent expansion energy (W_E or input heat) and the work-equivalent compression energy (W_C or output heat). The work equivalent energy per cycle ($W_{out} = W_E + W_C$) is then given by (P_{mean} is the standard atmospheric pressure of 1 atm = 101.35 kPasc):

$$W_{out} = [P_{mean} V_{SE} \pi C (1-t) \sin a]/[1+(1-C^2)^{0.5}] = 0.158 \text{ joules}$$

with an efficiency of:

$$\text{eff}_{\text{Carnot}} = W_{out}/Q_{in} = W_{out}/W_E = 1 - T_f/T_{in} = 1 - t = 0.06$$

The power of the work performed over time is then simply given by:

$$L_{\text{Schmidt}} = W_{out} \cdot \text{rps} = 0.3128 \text{ watts}$$

By the Schmidt model, then, an average motor speed of 118-120 rpm would constitute a power output of more than 310 milliwatts. If it were continuous, the work produced after 24 hours would be equivalent to the outflow of more than 27 kJ from the HYBORAC.

Experimental determination of the MM6 thermomechanical output power—preliminary determination of output power by gravity acceleration with a string-and-pulley method:

On a different MM6 of an earlier vintage (different shape and size small wheel, different regenerator materials and volumes, central shaft twice as large) the smaller "wheel" (radius of 0.0175 m) was completed with balsa inserts that added 0.8 gm, and calibrated weights attached to it with wire, with a total wire weight of 1.04 gm. The added weights of balsa and wire were, therefore, negligible. The balsa inserts were epoxied in place, and two wire guides—about 0.125-inch apart, serving as guides to prevent the ultra-fine nylon thread from slipping off—were attached to the small wheel. Friction through the hooks is also assumed to have been negligible (the suspension was threaded up toward the ceiling, then through two U-shaped nail hooks in the wood ceiling beam). The Stirling was rotated ("loaded") so that the small wheel wound up the nylon thread until the weight hung near the top hook. At $t = 0$, the larger wheel of the Stirling was released from the brake position and a digital stopwatch was activated. When the weight hit the surface, after a height of fall of 2.235 meters, the stopwatch was stopped. With this method, known as the string-and-pulley method,¹³ the test engine appeared to reach steady-state speeds with the 10 and 20 gm weights. Calibration data are shown in Table 1.

The formulas used were:

$$\text{rpm} = (1.22 \times 10^3)/t_{ff}$$

TABLE 1

Test mass	time (in sec)	rpm	power (mW)
5 gm	16.2	75.3	6.76
5 gm	18.6	65.4	5.87
5 gm	19.4	63.0	5.66
10 gm	9.86	124	22.3
10 gm	9.81	124	22.3
20 gm	6.35	192	69.0
20 gm	6.43	190	68.2
20 gm	6.24	195	70.0
100 gm	2.99	408	73.3

where t_{ff} is time of fall in seconds from the 2.235 m height, and for power:

$$L_{ff} = \text{torque} \cdot \text{angular speed} = m g (0.0175 \text{ m}) (2\pi \text{ rpm}/60) = m_{\text{test}} (1.8 \cdot 10^{-5}) \text{ rpm}$$

with m_{test} in grams. Temperature difference between the hot plates and cold plates of this Stirling was, at most, ca 0.5°C (with no heat applied to either plate).

Calibration of the MM6 (#2) output power with prony-brake dynamometers, in the HYBORAC/Stirling assembly.

Initial power calibration of the MM6 (#2) motor employed in the open-air HYBORAC studies above, was carried out with quadrant-gravity scales: the scale, suspended vertically, was calibrated with 5, 10, 20, and 100 gm certified brass weights, and then its hook was horizontally attached, via a strong cotton string, to a nipple (mean radius $r_n = 0.0053$ meters) built to fit the shaft of the Stirling engine. Speed measurements were taken before and after each dynamometer reading of the test mass value on the scale, with and without the nipple on the motor, and no significant differences were observed. The flywheel shaft will come to a stop when the power of the force of friction being exerted equals the output power of the shaft:¹³

$$L_{\text{dyna}} = m_{\text{test}} g r_n (2\pi \text{ rps})$$

This gives power directly in watts, with the test mass in kilograms; $g = 9.8065 \text{ N per meter}$.

The motor was set to the desired steady-state speed while driven from the HYBORAC, and the string was looped by hand two to four loops around the nipple before, on its own by friction, it instantly brought the motor to a stop—at which point, a peak reading on the quadrant scale was taken. Preliminary results were as shown in Table 2.

More accurate measurements were subsequently made with a pencil-type, spring-loaded prony-brake (absorption) dynamometer employing two scales, 0 to 100 gm, and 0 to 500 gm. The first was calibrated with 5, 10, 20, and 100 gm and the second with 20, 50, 100, and 500 gm certified brass weights. The scales were horizontally mounted at the height of the top surface of the nipple and the string ran directly from the nipple to their end. Care had to be exercised for the nipple mount not to exert friction on the shaft. The procedure was as described previously for the quadrant scale method, including measurement of motor speed before and after each test, with and without the putative nipple. The method of looping the string around the moving nipple takes great patience and some skill, and we found that moistening the hard rubber surface of the nipple permits a better traction for the looped string to arrest the motor.

The spring-loaded prony-brake dynamometer calibration

TABLE 2

Test mass (gm)	ΔT (°C)	rpm	power (mW)
35	6.6	64	12.2
>100	13.2	119	>64.8

was performed directly on the HYBORAC daytime assembly with the motor at steady state, while operating outdoors with typical ΔT values. The DWLS calibration curve for output power is shown in Figure 8a—six out of the eight points were means of $n = 3$ measurements, the other two were means of 2 measurements. Linear regression analysis of the data places an output of 57 mW at 100 rpm, 79-80 mW at 120 rpm, 86 mW at 123 rpm and 95-96 mW at 132.5 rpm (the daytime mean of the May 19 experiment), as shown in Figure 8b, with a slope of 1.15 mW per rpm. Peak output power tested was 175 mW at a speed of 187 rpm. The calibration of ΔT vs. motor rpm is shown, for the same experiment, in Figure 9, analyzed as linear regression with a slope of 6.7 rpm per °C of ΔT .

These results suggest that the Schmidt prediction is off by ca 4x from the experimental result, for the chosen comparison point (~120 rpm) situated midway through the calibra-

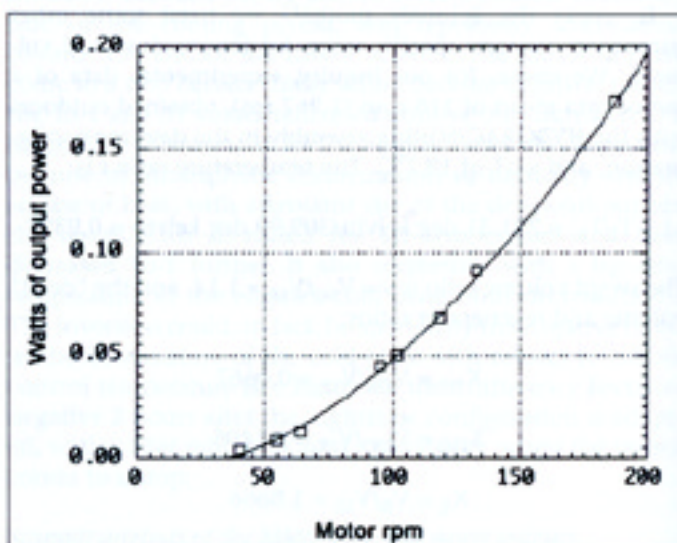


Figure 8a. Outdoor distance weighted least squares (DWLS) calibration curve for the MM6 (#2) Stirling motor output mechanical power as a function of motor rpm, while being driven by the HYBORAC.

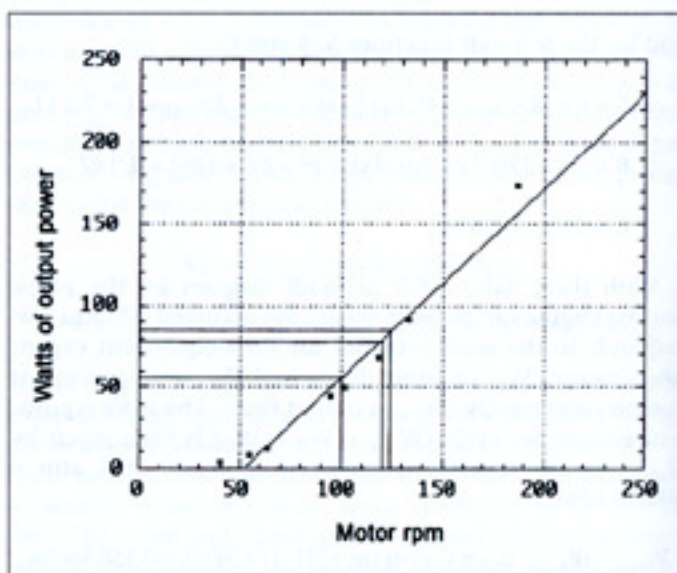


Figure 8b. Outdoor linear calibration curve for the MM6 (#2) Stirling motor output mechanical power as a function of motor rpm, while being driven by the HYBORAC.

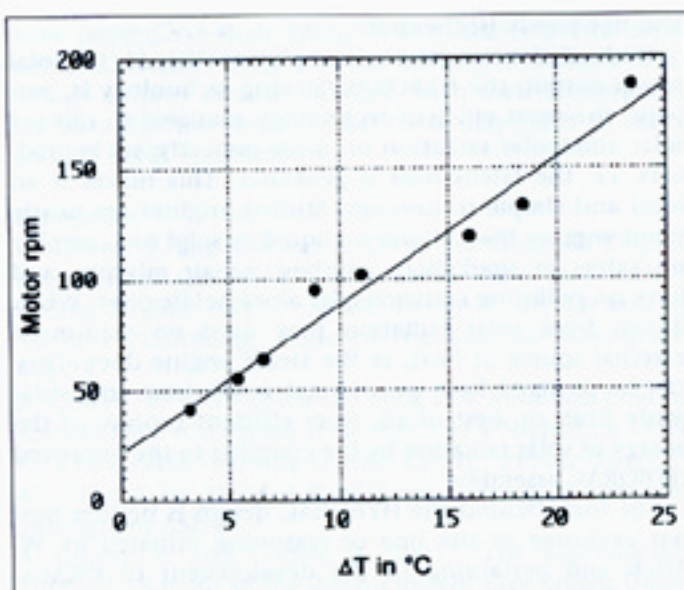


Figure 9. Outdoor linear calibration curve for the MM6 (#2) motor speed as a function of ΔT , while being driven by the HYBORAC.

tion curve (see Figure 8a). The results also cautioned us about the MM6 variability, underlining the necessity of testing throughout with the same motor and the impossibility of interchanging calibrations performed with different motors.

Calibrated power output from the May 19, 2003 experiment.

Linear regression analysis of the spring-loaded dynamometer calibration gave a slope of $S = 0.00115 \text{ W/rpm}$. However, this skews the values in the low range ($<50 \text{ rpm}$) of motor speed. Accordingly, we refined the calibration function as follows (where 0.006 W/rpm is the mean for low speed from the DWLS analysis in Figure 8a):

1. For speeds greater than 50 rpm:

$$I_{\text{dynamometer}} \text{ in watts} = (50 \text{ rpm} \times 0.0006 \text{ W/rpm}) + \{(S \text{ in W/rpm})(\text{rpm} - 50 \text{ rpm})\}$$

2. For speeds lower than 50 rpm:

$$I_{\text{dynamometer}} \text{ in watts} = (\text{rpm} \times 0.0006 \text{ W/rpm})$$

We next applied this to the analysis of the May 19 experiment for the HYBORAC configurations previously described.² The output power results are shown in Figure 10—with the daytime mean of 125 mW being sustained for 12 hours (a total daytime work of 5.4 kJ; with a mean of 95 mW, the total daytime work could be as low as 4.1 kJ), for a mean speed of 132.5 rpm.

Peak daytime output reached 165 mW. The nighttime mean of 25 mW was sustained for 8 hours (a total nighttime work of 0.72 kJ). The overall daytime and nighttime mean output power was $0.077 \text{ W} \pm \text{SEM } 0.01 \text{ W}$ ($n = 32$). The total work output in nearly 20.5 hours was 6.12 kJ. On an hourly basis, the daytime operation had an output at least 5x greater than the nighttime operation.

Comparison of the HYBORAC/Stirling technology to solar photovoltaic technologies.

We now compare the output power efficiency of photovoltaics to the thermomechanical output of the Stirling

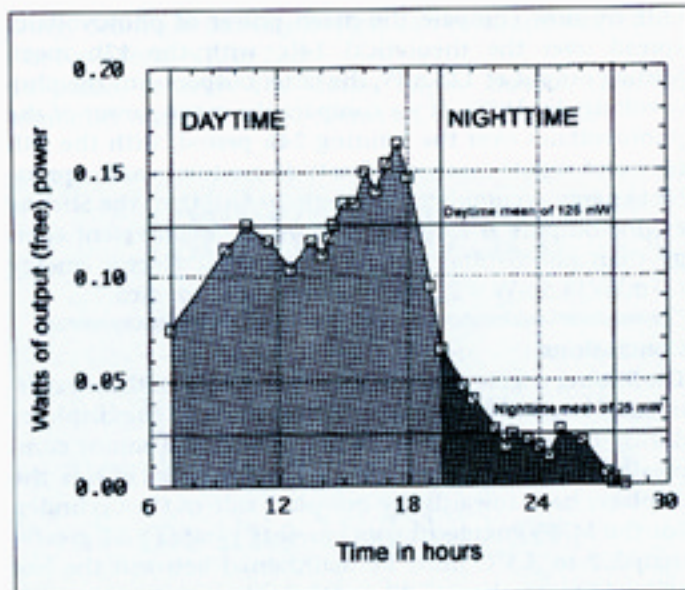


Figure 10. Calibrated mechanical output power of the Stirling MM6 (#2) during the 20.5 hours of the May 19, 2003 experiment.

engines being driven from the HYBORAC.

Typical photovoltaic films of amorphous silicon (e.g. Millenia™ produced by Solarex) can, on average, produce 4Wh per day per watt rating.¹⁴ A square meter of such photovoltaics would be able, in principle ("is rated"), to generate 163.2 Wh (587.5 kJ) per day. For the reference top-of-the-atmosphere surface solar radiation power constant of 1366 W m^{-2} (Reference 15) with a total daily energy of 32.78 kWh per square meter, the rated 0.16kWh to be captured per day, only constitutes an effective 0.48% efficiency. For an eight-hour period of solar radiation, and a total of 10.93kWh of energy, the efficiency figure (artificially) rises to 1.44%. This practical solar efficiency is, of course, less than the laboratory efficiency of crystalline solar cells, placed at 14%, and having a theoretical efficiency limit of 28%.¹⁶

Down in the atmosphere, at the Earth's surface, on a clear day, the zenith Sun will yield substantially less power than that of its power constant.¹⁷ At 45° N latitude (our location is at $43^\circ 41' \text{ N Lat}$), a surface of 1 square meter with a 45° slope, on June 22 (after the summer solstice), receives an average of 688 Langleys per day,¹⁸ or 28.785 million joules per day, with a total incident power of 333 watts per square meter. An effective surface of 0.0413 m^2 (a single face of the HYBORAC) under the same conditions will receive a maximum power of 13.76 watts, for a total incident energy—in a 14 hour day—of 693.5kJ, or 192.6Wh. An equal area photovoltaic would only produce

$$192.6\text{Wh} \times 0.0048 = 0.9245\text{Wh} = 3.328 \text{ kJ}$$

of electric energy. Moreover, this assumes that throughout those 14 hours the photovoltaics were mounted on a solar tracker to keep that 45° slope constant (for purposes of comparison with the 45° slope of the HYBORAC face with respect to the sun). Spread over the 14 hours of solar exposure, this corresponds to a mean power of 66 mW and spread over the 24 hours of the day, it corresponds to a mean of 38.5 mW.

If we now compare the mean power of photovoltaics spread over the theoretical 14h, with the 12h mean Stirling output of 125 mW, the latter outperforms the photovoltaics by 189%. If we compare the mean power of the photovoltaics over the limiting 24h period, with the 24h (day and night) mean of 77 mW (for a total work-equivalent energy accumulated through 20.5h), then the Stirling engine outputs at least 200% more work-equivalent energy than photovoltaics effectively output electric energy ($77\text{mW}/38.5\text{mW} = 2$), for the same collector area.

Conclusions

The Stirling engine is a two-pulse hot gas (air in these experiments) engine, with an expansion pulse of the displacer during the heating phase of the cycle and a minor compression pulse during the cooling phase that forces the displacer back towards the hot-plate side of the cylinder. For the MM6 engine to continuously rotate, a ΔT greater than 3.2 to 3.5°C must be maintained between the hot and cold plates, irrespective of their absolute temperature. By our estimates, this requires a thermal power influx minimum of ca 250 to 300 mW, that outputs a scant <2 mW of power.

With a Carnot efficiency of 6%, the mean daytime mechanical output power of 125 mW requires effective provision (by the HYBORAC) of at least 2.08 watts of continuous sensible thermal power to the Stirling hot-plate—more than 100x the power of the sensible thermal flux measured as transiting through these boxes, and in accordance with the kinetic theory of heat. For the 20.5 hour experimental mean of 77 mW, and a Carnot efficiency near 4.3%, the HYBORAC must provide a mean sensible thermal power of ca 1.75 watts; and for the mean nighttime mechanical output power of 25 mW, with an efficiency near 1.6%, the HYBORAC must provide a sensible thermal flux of at least 1.5 watts. When considering the HYBORAC, where do these tremendous quantities of sensible heat come from? That is the question we shall address in the companion report—and which we now suggest must come from the latent heat accumulated by the HYBORAC through its capture of solar ambipolar energy. If we can experimentally confirm these values for the HYBORAC output that feeds the Stirling hot plate, then the combined efficiency of the HYBORAC at capturing solar radiation and releasing sensible heat may be as high as 200% that of passive solar collectors.

In trying to understand the properties of the Stirling engine, it is a useful exercise to analyze the reasons why Schmidt theory cannot accurately predict the power output of these engines. Schmidt theory assumes 1) that there is no pressure loss in the heat exchangers and there are no internal pressure differences, 2) that the expansion and compression processes are isothermal, 3) that the working gas behaves as an ideal gas, 4) that perfect regeneration takes place, 5) that the “dead space” volumes (of expansion and compression) are isothermal in their respective phases, 6) that the regenerator temperature is an average given by $T_R = (T_{in} + T_f)/2$, and 7) that the expansion and compression volumes behave according to a sine curve.¹² However, there are internal pressure differences at work, and like differences also in the heat exchangers. The compression and expansion phases are

also not purely isothermal.

With efficiencies greater than photovoltaic for the total power output, the HYBORAC/Stirling technology is, perhaps, the most efficient technology available to capture solar ambipolar radiation or, more correctly, its byproducts, i.e. the latent heat it generates. This makes it an ideal and simple technology. Stirling engines are nearly silent engines that require no liquid or solid fuel, employ no valves or sparkplugs, combust no air mixture, and have no polluting emissions, let alone acidic ones. When driven from solar radiation they need no man-made external source of heat, as the steam engine does. They can be powered from geothermal vents, from industrial waste heat, or, best of all, from efficient capture of the energy of solar radiation by the coupling to the improved HYBORAC assembly.

The logic behind the HYBORAC design is neither new nor exclusive to the line of reasoning initiated by W. Reich and pertaining to the development of ORACs, BORACs, and HYBORACs. Back in the early 1930s, hot-air engines were used in remote areas to power fans from black-coated cylindrical heat reservoirs designed for solar exposure.¹⁹ What makes the improved HYBORAC design so special is its high efficiency of capture of the byproducts of solar radiation, specifically latent heat.

Our next objective is twofold: 1) to increase the nighttime performance so that it eliminates the observed inversion of T_o - T and ΔT , and becomes comparable to the daytime performance; 2) to raise the overall performance so that the HYBORAC will have enough power to drive the Stirling engine around the clock. Experiments that succeeded in accomplishing these tasks and achieved around-the-clock performance and comparable day and night power outputs, for two full days (but in principle easily extendable for much longer periods, if not indefinitely), will be reported on shortly. (See monograph already posted on www.aetherometry.com.)

For purposes of comparison with one other prominent aspiring new energy source, the Stirling/HYBORAC technology in these experiments produces mechanical output power directly, whereas LENR “cold fusion” cells have produced so far only thermal excess power even when the “heat-after-death” (zero input power) phenomenon appears. Also, the mechanical output power (only against friction, for now) in these preliminary non-optimized devices is comparable in magnitude or even greater than the thermal excess power in many typical (but certainly not all) experimental LENR/cold fusion cells.

This is a concrete demonstration of the energy reservoir of the cosmic energetic aether, as sourced (in this application) in the Sun, but going beyond the heretofore incomplete physical models, such as the commonly understood “solar electromagnetic spectrum.” It would involve some difficulty to come up with a simpler, cleaner, safer and quieter passive form of collection of a power that is “free for the taking,” than the HYBORAC/Stirling combination. The aim of our next report will be to discuss our already achieved increased performance of this technology—greater and continuous round-the-clock power outputs.

Finally, we must remark that this demonstration technology is by no means the full extent of possible aether energy technology, as the first two authors of this paper

have proved via their PAGD™ and Aether Motor technologies. Neither these nor the Stirling/HYBORAC technology employ nuclear changes, with their accompanying hazards, however minimal these may seem in many present LENR experiments.

References

1. Correa, P. and Correa, A. 2002. "A Modified Orgone Accumulator (HYBORAC) as a Drive for a Low delta-T Stirling Engine, Part I," *Infinite Energy*, 7, 41, 23; also by Akronos Publishing, Concord, Canada, as Monograph AS2-25.
2. Correa, P. and Correa, A. 2002. "A Modified Orgone Accumulator (Complete HYBORAC) as a Nighttime Drive for a Low delta-T Stirling Engine, Part II," *Infinite Energy*, 7, 42, 41; also by Akronos Publishing, Concord, Canada, as Monograph AS2-26.
3. Correa, P. and Correa, A. 2001. "The Reproducible Thermal Anomaly of the Reich-Einstein Experiment Under Limit Conditions," *Infinite Energy*, 2, 7, 12.
4. Reich, W. 1947-1951. *The Cancer Biopathy*, 1973 ed., Farrar, Straus & Giroux, New York, NY, p. 89.
5. *Idem.*, p. 123.
6. *Idem.*, pp. 87, 89.
7. Correa, P. and Correa, A. 2001. "To Be Done with (An)orgonomists: Conversations with (hopefully!) the Last One: A Complete Response to J. DeMeo's Attack on Aetherometry," at www.aetherometry.com/tobedone.html.
8. Correa, P. and Correa, A. 1998, 2001. "The Thermal Anomaly in ORACs and the Reich-Einstein Experiment: Implications for Blackbody Theory," Akronos Publishing, Concord, Canada, Monograph AS2-05.
9. Correa, P. and Correa, A. 1999, 2001. "The Indirect 'Orgone Effect' of Tesla Radiation: Ambipolar Aether and Blackbody Radiation Spectra," Akronos Publishing, Concord, Canada, Monograph AS2-17A.
10. Correa, P. and Correa, A. 2000. "Determination of the OR and DOR Energies, Frequencies, and Wavelengths Driving the Atmospheric Allotropic Cycle of Oxygen, Ozone, and Water," Akronos Publishing, Concord, Canada, Monograph AS2-17B.
11. Correa, P. and Correa, A. 1998, 2001. "Comparative Study of the Variation in the Spontaneous Discharge Rate of Atmospheric Electroscopes and Electroscopes Placed Within 'Orgone Accumulators,'" Akronos Publishing, Concord, Canada, Monograph AS2-06.
12. Hirata, K. 1997. "Schmidt Theory for Stirling Engines," at www.bekkoame.ne.jp.
13. Veinott, C.G. 1973. "Fractional—and Subfractional—Horsepower Electric Motors," McGraw-Hill Book Co, New York, NY, pp. 390-392.
14. "Solar power short course," Key Telemetering Products, Owensboro, KY, at <http://www.keytelemetering.com/tutorial.html>.
15. Foukal, P. and Lean, J. 1990. "An Empirical Model of Total Solar Irradiance Between 1874 and 1988," *Science*, 247, 556.
16. Hamakawa, Y. 1987. "Photovoltaic Power," *Scientific American*, April, 87.
17. Flohn, H. 1969. *Climate and Weather*, World University Library, McGraw-Hill Book Co, New York, NY, p. 26.
18. Davis, A. and Schubert, R. 1977. *Alternative Natural*

Energy Sources in Building Design, Van Nostrand Reinhold Co, New York, NY, p. 223.

19. Rizzo, J. 1999. *The Stirling Engine Manual*, Camden Miniature Steam Services, Somerset, England, p. 2.